crystals

MDPI

Article

Salts of S-(+)-Ibuprofen Formed via Its Reaction with the Antifibrinolytic Agents Aminocaproic Acid and Tranexamic Acid: Synthesis and Characterization

Hannah M. Frösler, Humbelani S. Ramulumo, Cesarina Edmonds-Smith and Mino R. Caira *

Centre for Supramolecular Chemistry Research, Department of Chemistry, University of Cape Town, Rondebosch 7701, South Africa; frshan001@myuct.ac.za (H.M.F.); humbelani.ramulumo@alumni.uct.ac.za (H.S.R.); c.edmonds-smith@uct.ac.za (C.E.-S.)
* Correspondence: mino.caira@uct.ac.za; Tel.: +27-21-650-3071

Abstract: The paucity of multi-component compounds containing the non-steroidal anti-inflammatory drug (NSAID) S-(+)-ibuprofen (S-IBU) in combination with other drugs prompted the present study, which describes 1:1 salts of this active pharmaceutical ingredient (API) with the two most widely used antifibrinolytic APIs, namely 6-aminohexanoic acid (aminocaproic acid, ACA) and tranexamic acid (TXA), which are zwitterions in the solid state. Since NSAIDs are known to cause adverse side effects such as gastrointestinal ulceration, the presence of ACA and TXA in the salts with S-(+)-ibuprofen might counter these effects via their ability to prevent excessive bleeding. The salts were prepared by both the liquid-assisted grinding method and co-precipitation and were characterized by X-ray powder diffraction and single-crystal X-ray diffraction, thermal analysis, Fourier transform infrared spectroscopy, and solubility measurements. The X-ray analyses revealed a high degree of isostructurality, both at the level of their respective asymmetric units and in their extended crystal structures, with charge-assisted hydrogen bonds of the type $N\text{-}H^{+}\cdots O^{-}$ and $O\text{-}H^{+}\cdots O^{-}$ featuring prominently. The thermal analysis indicated that both salts had significantly higher thermal stability than S-(+)-ibuprofen. Solubility measurements in a simulated biological medium showed insignificant changes in the solubility of S-(+)-ibuprofen when tested in the form of the salts $(S\text{-}IBU)^{-}(ACA)^{+}$ and $(S\text{-}IBU)^{-}(TXA)^{+}$.

Keywords: S-(+)-ibuprofen; dexibuprofen; antifibrinolytics; aminocaproic acid; tranexamic acid; salt formation; X-ray diffraction; thermal analysis; spectroscopy; solubility

Citation: Frösler, H.M.; Ramulumo, H.S.; Edmonds-Smith, C.; Caira, M.R. Salts of S-(+)-Ibuprofen Formed via Its Reaction with the Antifibrinolytic Agents Aminocaproic Acid and Tranexamic Acid: Synthesis and Characterization. *Crystals* **2023**, *13*, 1222. https://doi.org/10.3390/cryst13081222

Academic Editors: Duane Choquesillo-Lazarte and Alicia Dominguez-Martin

Received: 4 July 2023
Revised: 31 July 2023
Accepted: 3 August 2023
Published: 8 August 2023

1. Introduction

The crystal engineering of multi-component solids containing active pharmaceutical ingredients (APIs), manifested as crystalline drug solvates, cocrystals, ionic cocrystals, molecular salts, eutectic mixtures, inclusion complexes, fixed-dose formulations composed of two or more APIs, and amorphous combinations, has burgeoned in recent years owing to the potential or proven utility of such new compounds in the medicinal context. The authors of a recent editorial in the present journal [1], announcing the first volume of the Special Issue on this subject, affirmed that research on such multi-component solids is a 'hot' topic, and they duly listed several therapeutically effective cocrystals that have been approved by leading international regulatory agencies and subsequently commercialized.

In this report, we highlight the preparation and physicochemical characterization of two new multi-component compounds containing the eutomer of the non-steroidal anti-inflammatory drug (NSAID) ibuprofen (2-(4-isobutylphenyl)propanoic acid, Figure 1a), which has potent antipyretic, analgesic, and anti-inflammatory properties and is used in the treatment of pain, acute inflammation, and fever [2,3]. A survey of the literature revealed numerous reports on multi-component compounds containing both racemic ibuprofen and the eutomer S-(+)-ibuprofen (also known as dexibuprofen), the latter being

the more therapeutically active enantiomer than the R-(-)-enantiomer, displaying 160-fold higher activity as an inhibitor of prostaglandins, which are associated with fever and inflammation [2].

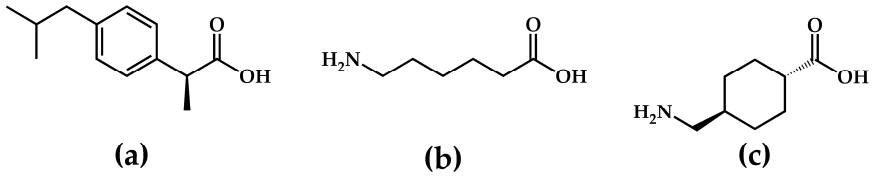

Figure 1. The chemical structures of the APIs S-(+)-ibuprofen (**a**), ε-aminocaproic acid (**b**), and tranexamic acid (**c**).

Furthermore, although the administration of racemic ibuprofen results in the inactive R-(-)-enantiomer being metabolized to the S-(+)-enantiomer, the extent of this process varies amongst patients, leading to anomalies in patient dose–effect responses [2,3]. Thus, given the potent activity and 'cleaner' metabolism of S-(+)-ibuprofen, as well as its somewhat reduced level of undesirable gastric side effects compared with the R-(-)-enantiomer [4], there are significant advantages in employing this solid form of ibuprofen as the principal API in multi-component systems. A summary of such previously reported systems follows, with an emphasis on pharmaceutically relevant crystalline phases, a topic that has recently been comprehensively reviewed [5].

Despite the very poor aqueous solubility of S-(+)-ibuprofen (<0.1 mg/mL at 25 °C) [6], relatively few cocrystals containing this API have been fully characterized and exploited for solubility improvement. In an early study [7], cocrystal formation via liquid-assisted grinding (LAG) with the well-known water-soluble coformer nicotinamide was established by powder X-ray diffraction (PXRD), the authors noting an increase in the melting point of the product effected by co-crystallization. Subsequently, the X-ray structure determination of the cocrystal was determined using synchrotron radiation [8]. A more recent pharmaceutically relevant report referred to cocrystals formed between S-(+)-ibuprofen and each of the coformers benzamide and picolinamide [9], but no reference to a resulting property enhancement was evident. The authors of a recent detailed study of cocrystal formation between chiral compounds [10] reported a rare example of a 'drug–drug' cocrystal containing S-(+)-ibuprofen and the novel chiral antiepileptic agent levetiracetam ((S)-2-(2-oxopyrrolidin-1-yl)butanamide).

Salts containing the S-ibuprofenate ion and counter cations have also been developed for improved performance in the delivery of APIs. Such salts generally display improved solubility profiles relative to untreated APIs. Recently reported X-ray structures of representative salts appearing in the Cambridge Structural Database (CSD) [11] include piperazinediium bis(S-(+)-ibuprofenate) (refcode FAGKAD01) and (S)-1-phenylethylammonium (S)-ibuprofen (VAKVEK01). A more detailed summary of known cocrystals and salts derived using S-(+)-ibuprofen as an API can be found in a recent paper [12].

Still more relevant in the context of the study reported in the present paper are binary products obtained by the reaction of APIs with zwitterions as coformers [13]. From the X-ray structure of the crystalline product containing S-(+)-ibuprofen and the amino acid proline, determined from powder diffraction data, the API was evidently in its neutral state [14], whereas in the salt formed with arginine [12], the single crystal X-ray structure indicated that the API was deprotonated. The clinical properties of the latter product (ibuprofen arginate), including its advantage of rapid-onset pain relief, have been reviewed [15].

Given the paucity of reported multi-component 'drug–drug' combinations containing S-(+)-ibuprofen, the aim of the present study was the synthesis and physicochemical characterization of products obtained by the reaction of S-(+)-ibuprofen with both ε-aminocaproic acid (6-aminohexanoic acid) and tranexamic acid (trans-4-(aminomethyl)cyclohexanecarboxylic acid) (Figure 1b,c). These APIs are zwitterionic in the solid state [11]. One novel aspect of this study is that these coformers are two of the most widely used antifibrinolytic drugs,

being highly effective in reducing or preventing blood loss (potentially including gastric and intestinal bleeding) by arresting the breakdown of blood clots (fibrinolysis) via their reversible binding to plasminogen. Detailed accounts of their mechanisms of action have appeared in recent reviews [16–18].

A CSD search for multi-component structures containing the API ε-aminocaproic revealed only those of the dihydrogen phosphate salt (refcode JIZHEF) and the hydrated tetraphenylborate salt (CSD refcode QEGFIR). However, X-ray structures of salts and co-crystals obtained by the reaction of the API tranexamic acid with a series of carboxylic acid coformers have recently been reported [19], two of which are rare examples of 'drug–drug' salts containing the salicylate and 2,5-dihydroxybenzoate anions, each in association with the TXA cation, whose terminal groups are NH_3^+ and COOH.

Given that the administration of S-(+)-ibuprofen is known to cause some level of gastric side effects such as ulceration, bleeding, and the perforation of the stomach lining [4], the presence in the same multi-component crystal of both an NSAID and these antifibrinolytic agents in the new salts reported here could conceivably reduce such undesirable effects. Each of the two new products reported here is a 1:1 salt containing deprotonated S-(+)-ibuprofen and the respective protonated antifibrinolytic agent. These compounds can thus be considered as potential fixed-dose 'drug–drug' combinations, with the ability to treat inflammation, fever, and analgesia, with a simultaneous reduction in gastrointestinal damage. The salts were prepared by liquid-assisted grinding (LAG) and co-precipitation methods and were subsequently analyzed by X-ray powder diffraction (PXRD), thermogravimetric analysis (TGA), differential scanning calorimetry (DSC), Fourier transform infrared (FT-IR) spectroscopy, single-crystal X-ray diffraction (SCXRD), and solubility measurements in a simulated biologically relevant medium. An interesting feature of the crystal structures of the salts, namely isostructurality, was revealed by SCXRD. The following abbreviations are used henceforth for naming the APIs: S-(+)-ibuprofen (S-IBU), ε-aminocaproic acid (ACA), and tranexamic acid (TXA).

2. Materials and Methods

2.1. Materials

S-IBU, ACA, and TXA were purchased from Sigma-Aldrich (Cape Town, South Africa) and were used without further purification. Common solvents employed in liquid-assisted grinding and co-precipitation experiments (methanol, ethanol, isopropanol, and acetonitrile) were purchased from Thermo Fisher Scientific (Johannesburg, South Africa) and were of analytical grade.

2.2. Synthesis via Liquid-Assisted Grinding and Co-Precipitation

To assess the affinity of S-IBU for reaction with the zwitterionic coformers ACA and TXA, physical mixtures containing S-IBU (5 mg, 0.024 mmol) and the molar equivalent of each of the coformers ACA and TXA were subjected to liquid-assisted grinding (LAG) for 15–20 min. with the continual addition of several microliters of the selected solvent. Solvents were added in 20 μL aliquots every minute on average. With coformer ACA, the total volumes added (in μL) were 620 (MeOH), 580 (EtOH), and 680 (MeCN). With coformer TXA, the corresponding volumes were 680, 740, and 660 μL. Single crystals of the products were isolated by co-precipitation, which involved the dissolution of S-IBU and each of ACA and TXA in equimolar amounts via a common solvent in separate vials using a hot-plate and magnetic stirring at a temperature approximately 10 °C lower than the boiling point of the solvent. This was followed by mixing each coformer solution with a solution of S-IBU, and the resulting solutions were stirred at the same constant temperature for ~1 h and finally filtered into clean vials using 0.45 μm nylon filters. The crystals of the products were collected after several days.

2.3. X-ray Powder Diffraction

The PXRD patterns of the products obtained by LAG were recorded on a Bruker D2 Phaser desktop powder diffractometer (Billerica, MA, USA) and compared with those of the starting components to determine whether new phases had been generated. CuKα_1 radiation (λ = 1.5406 Å) was employed, with generator settings of 30 kV, 10 mA. To minimize the preferred orientation, the samples were gently ground, placed on a rotating silicon zero-background sample holder, and scanned (range 5–40° 2θ, step size 0.0164°).

2.4. ^{1}H-NMR Spectroscopy

To determine the stoichiometries of the two salts of S-IBU, their proton NMR spectra were recorded in deuterated N,N′-dimethylsulfoxide (DMSO-d_6) on a Bruker Ultrashield 400 Plus Spectrometer (Billerica, MA, USA).

2.5. Single-Crystal X-ray Diffraction (SCXRD)

Intensity data for the S-IBU·ACA and S-IBU·TXA crystals were collected on a Bruker Kappa APEX II DUO single-crystal X-ray diffractometer and a Bruker D8 Venture diffractometer, respectively, with MoKα radiation (λ = 0.71073 Å) and with both crystals cooled to 100(2) K. Details of their structure solutions and refinements and the relevant software employed are fully listed in the respective Crystallographic Information Files (CIFs). In particular, the determination of the precise nature of these compounds was confirmed by (inter alia) the careful location of hydrogen atoms to indicate unequivocally whether they were salts or cocrystals. Non-hydrogen atoms were refined anisotropically, and the H atoms, after location on Fourier maps, were included in idealized positions in a riding model with isotropic thermal displacement parameters.

2.6. Thermal Analysis

The thermal stability of the products was investigated by thermogravimetric analysis (TGA) and differential scanning calorimetry (DSC) using a TA-Q500 (New Castle, DE, USA) instrument and a TA Discovery DSC 25 instrument (New Castle, DE, USA), respectively, with a common heating rate of 10 K/min. The purge gas was dry nitrogen flowing at 60 mL/min in each case. Samples (mass range 0.7–2.0 mg) were placed in an alumina crucible for TGA and in crimped platinum pans for DSC analysis.

2.7. Fourier Transform Infrared (FT-IR) Spectroscopy

Spectra in the range 4000–400 cm^{-1} were recorded on a PerkinElmer Spectrum Two instrument (32 accumulations, spectral resolution 4 cm^{-1}). The instrument was fitted with an attenuated total reflectance (ATR) attachment (Waltham, MA, USA).

2.8. Solubility Measurements

The medium for solubility measurements was FaSSIF (fasted-state simulated intestinal fluid) purchased from Biorelevant.com Ltd. (London, UK). It was prepared from FaSSIF/FeSSIF/FaSSGF powder, which was dissolved in phosphate buffers with pH values of 2.0 and 6.5. The solutions were used within 24 h after preparation. The composition of the FaSSIF was 105.7 mM sodium chloride, 28.7 mM sodium phosphate, and 10.5 mM sodium hydroxide. The equilibrium solubility was determined by adding an excess amount of S-(+)-ibuprofen, ACA, and TXA to 1 cm^3 of FassiF in a polytop vial. The solution was stirred at 25 $\pm$ 0.5 °C and 500 rpm. After 72 h, the solution was filtered through a 0.45 µm nylon filter. Each solution was diluted to be within the detection limits of the high-performance liquid chromatography (HPLC) system using MilliQ H_2O. An Agilent 1220 Infinity LC system was employed for the assays. The HPLC equipment included a binary pump with a sample degasser, autosampler, temperature-controlled column oven, and UV/VIS variable-wavelength detector. Data were collected and analyzed using Agilent ChemStation. Chromatographic separation was achieved on an Agilent Poroshell 120 EC-C_{18} (4.6 mm $\times$ 50 mm) with a 2.7 µm particle size column in gradient elution mode. Fifty

millimolar phosphate buffer (pH 7.5) and methanol were used as the mobile phase at a flow rate of 0.8 mL/min. The injection volume was 10.0 µL, and the eluents were monitored at 220 nm with the UV detector. The total chromatographic run period was 15.0 min. A calibration curve and the gradient elution program employed are included in the Supplementary Materials (Figure S1 and Table S1).

3. Results and Discussion

3.1. Synthesis and Characterization of the Products by XRD Methods and ^{1}H-NMR Spectroscopy

Following the LAG experiments described in Section 2.2, the co-ground products were investigated by PXRD. Figure 2 shows that with S-IBU and ACA as the starting materials, the same new crystalline phase was consistently obtained with the three different solvents for LAG, and that this common PXRD pattern differed very significantly from those of the starting components.

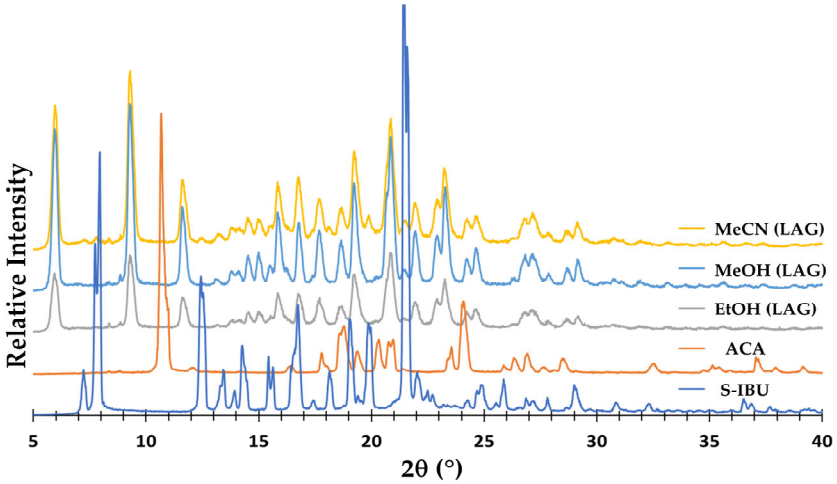

Figure 2. PXRD patterns of the starting components S-IBU and ACA, and those of the products obtained by liquid-assisted grinding using three solvents.

Analogous and consistent results were observed when S-IBU and TXA underwent LAG with the same solvents (Figure S2, Supplementary Materials). However, it was also observed that the new common crystalline phase produced in these experiments displayed major PXRD peaks in similar angular positions to those shown for the products in Figure 2. It was therefore evident that despite the different chemical structures of ACA and TXA, their products with S-IBU displayed some level of crystal isostructurality.

Single crystals of the two products obtained by the co-precipitation method were subsequently used for SCXRD and thermal analyses. The ^{1}H-NMR spectra of solutions of these crystals in DMSO-d_6 were recorded, and that for the salt with ACA indicated 1:1 stoichiometry. For the salt with TXA, however, stoichiometric variability was observed due to solubility issues, but the same 1:1 stoichiometry was rationalized from XRD and thermal analysis data (see below). SCXRD analyses indicated that the products were salts containing the S-(+)-ibuprofenate anion $(C_{13}H_{17}O_2)^-$ and the respective ACA and TXA counter cations, their terminal groups being NH_3^+ and COOH, as observed for the salicylate and 2,5-dihydroxybenzoate salts with TXA [19]. The systematic names for these new salts were, accordingly, 6-ammonio-*n*-hexanoic acid (2S)-2-(4-isobutylphenyl)propionate and (4-carboxycyclohexyl)methylammonium (2S)-2-(4-isobutylphenyl)propanoate, and their relevant crystallographic parameters are presented below.

Crystal data for $(S\text{-IBU})^-(ACA)^+$, $(C_{13}H_{17}O_2)^-$ $(C_6H_{14}NO_2)^+$ (M = 337.45 g/mol): monoclinic; space group $P2_1$ (no. 4); a = 15.0079(7) Å; b = 6.7425(3) Å; c = 19.2543(10) Å; β = 97.017(2)°; V = 1933.76(16) Å^3; Z = 4; T = 100(2) K; µ(MoKα) = 0.080 mm^{-1}; D_{calc} = 1.159 g/cm^3; 34,494 reflections measured (4.8° ≤ 2θ ≤ 54.3°); 8562 unique

(R_{int} = 0.0657, R_{sigma} = 0.0706), which were used in all calculations. The final R_1 was 0.0639 ($I > 2\sigma(I)$), and the final wR_2 was 0.1341 (all data).

Crystal data for $(S\text{-IBU})^-(TXA)^+$, $(C_{13}H_{17}O_2)^-$ $(C_8H_{16}NO_2)^+$ (M = 363.48 g/mol): monoclinic; space group $P2_1$ (no. 4); a = 15.623(5) Å; b = 6.687(2) Å; c = 20.571(6) Å; β = 99.867(12)°; V = 2117.3(11) $Å^3$; Z = 4; T = 100(2) K; μ(MoKα) = 0.078 mm^{-1}; D_{calc} = 1.140 g/cm^3; 41,905 reflections measured ($4.0° \leq 2\theta \leq 51.8°$); 8052 unique ($R_{int}$ = 0.0694, R_{sigma} = 0.0524), which were used in all calculations. The final R_1 was 0.0878 ($I > 2\sigma(I)$), and the final wR_2 was 0.2074 (all data).

As indicated in the recent article on salts and cocrystals containing TXA [19], given that TXA exists as a zwitterion in the solid state, predicting the outcome of its attempted co-crystallization with coformers is not straightforward. Nonetheless, applying the usual criterion involving ΔpKa (defined as pKa (base)–pKa (acid)), with pKa (base) = 10.2 for the amino group of TXA, and pKa (acid) being that of the respective coformer, the authors of the published study observed that all ΔpKa values exceeded 4, indicating a preference for salt formation. In the present case, with ACA and TXA having pKa (base) values of 10.8 and 10.2, respectively, and S-IBU having a pKa (acid) value of 4.4, analogous treatment yielded ΔpKa values exceeding 6, which was again consistent with salt formation.

Given that the salts crystallized in the same space group with very similar unit cell dimensions, both the common 1:1 stoichiometry and the prediction of some level of isostructurality between them from their PXRD patterns were vindicated. These features are evident from Figure 3, in which the two unit cells and their respective asymmetric units (ASUs) are shown from the same viewpoint. In each unit cell, the two crystallographically distinct S-IBU anion–counterion pairs are labelled AA and BB, with each ASU featuring a large cyclic hydrogen-bonded motif. Salt formation resulted from the deprotonation of the carboxylic acid group of the S-IBU molecule, with both cations having terminal ammonium and carboxylic acid groups. It was also evident that the isostructural arrangements of the ASUs (Figure 3) were favored by the conformations adopted by the cations, resulting in their very similar intramolecular $N^{(+)}\cdots$(terminal)O lengths in the ACA (7.75 and 7.83 Å) and TXA (7.37 and 7.38 Å) cations, and hence their consequent engagement in the same set of charge-assisted $N\text{-}H^{(+)}\cdots O^{(-)}$ and $O\text{-}H^{(+)}\cdots O^{(-)}$ hydrogen bonds [20] linking anions and cations.

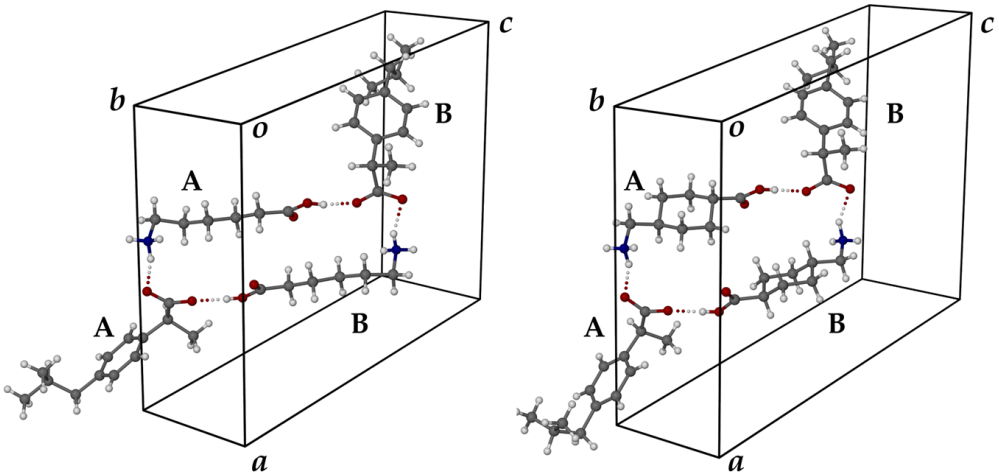

Figure 3. The ASUs of the salts $(S\text{-IBU})^-(ACA)^+$ (**left**) and $(S\text{-IBU})^-(TXA)^+$ (**right**).

For these unique charge-assisted $N\text{-}H^{(+)}\cdots O^{(-)}$ and $O\text{-}H^{(+)}\cdots O^{(-)}$ hydrogen bonds, the salient parameters are shown in Table 1.

Table 1. Charge-assisted H-bond parameters for ions in the ASUs of the salts.

SALT	N···O/Å	N-H···O/°	O···O/Å	O-H···O/°
$(S\text{-}IBU)^-(ACA)^+$	2.764(4)	164	2.565(4)	172
	2.857(4)	159	2.611(4)	177
$(S\text{-}IBU)^-(TXA)^+$	2.756(6)	160	2.622(6)	178
	2.847(7)	151	2.576(6)	175

The extent of overlap in the ASUs of the two salts is evident from the stereoscopic view in Figure 4.

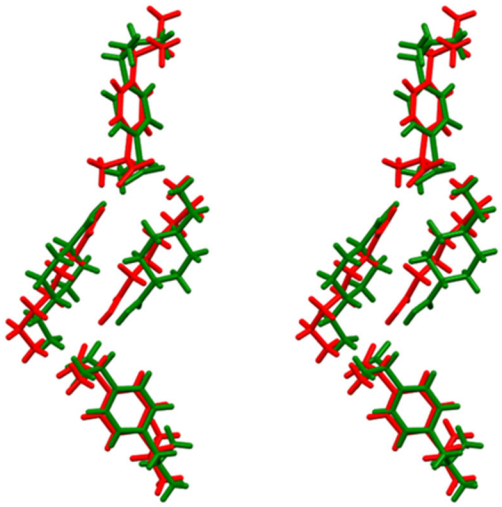

Figure 4. Stereoscopic view of the overlap in the ASUs of the salts with ACA (red) and TXA (green).

The N-H groups and O atoms in the cyclic motifs of both crystal ASUs (Figure 3) are donors and acceptors, respectively, in charge-assisted H-bonding with symmetry-related ring motifs, resulting in the formation of dense networks of H-bonds that stabilize these crystalline phases. The close isostructurality of the extended structures of the two salts is evident in the packing diagram (Figure 5).

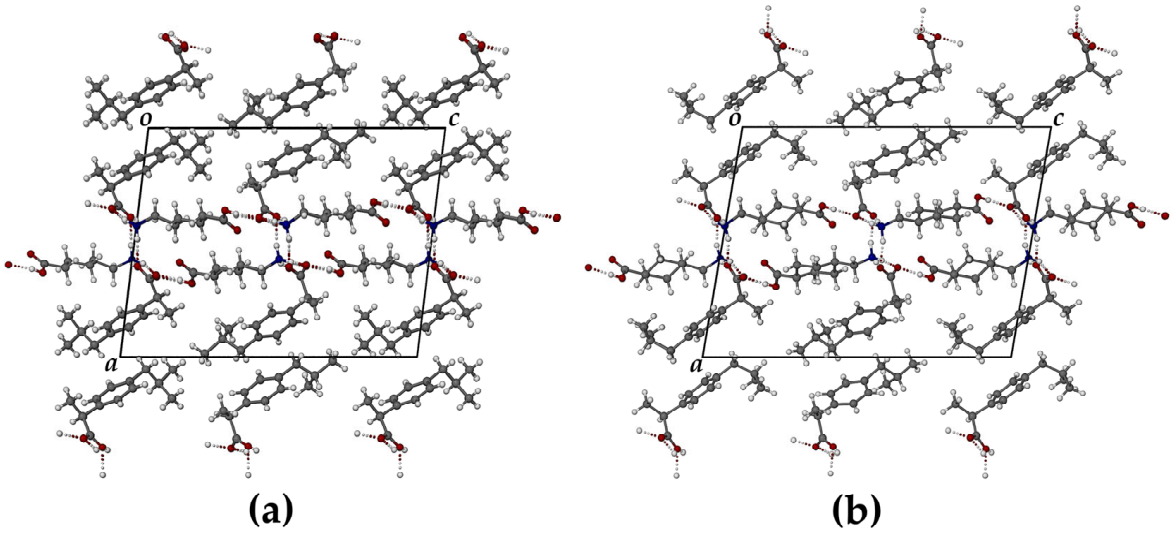

Figure 5. The [010] projection of the crystal packing in $(S\text{-}IBU)^-(ACA)^+$ (**a**) and $(S\text{-}IBU)^-(TXA)^+$ (**b**).

The experimental PXRD pattern for $(S\text{-}IBU)^{-}(ACA)^{+}$ and that calculated from the refined SCXRD data are shown in Figure 6. The correlation was reasonable, allowing for small differences in peak angular displacements due to the significantly different temperatures at which the two patterns were recorded (viz., 294 K and 100 K, respectively). Due to the large temperature difference of 194 K, the apparently significant differences in the two PXRD profiles at around 21 and 23° 2θ were attributed to small shifts caused by crystal anisotropy that seemed to 'split' each peak at these angular positions, producing 'doublet' peaks in the calculated PXRD pattern. Similar results were obtained for $(S\text{-}IBU)^{-}(TXA)^{+}$ (Figure S4).

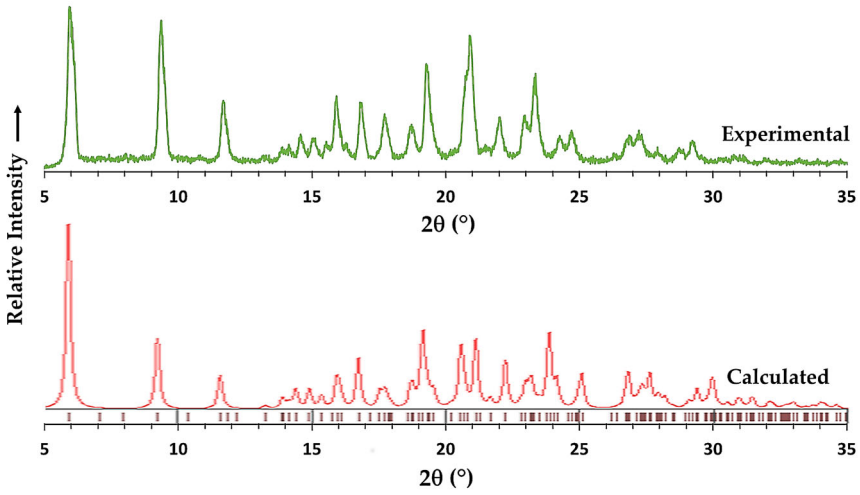

Figure 6. Experimental and calculated PXRD patterns for $(S\text{-}IBU)^{-}(ACA)^{+}$.

3.2. Fourier Transform Infrared (FT-IR) Spectroscopy

The FT-IR spectra of S-(+)-ibuprofen, the coformer ACA, and the resulting product shown in Figure 7 were consistent with the crystallographic findings for $(S\text{-}IBU)^{-}(ACA)^{+}$.

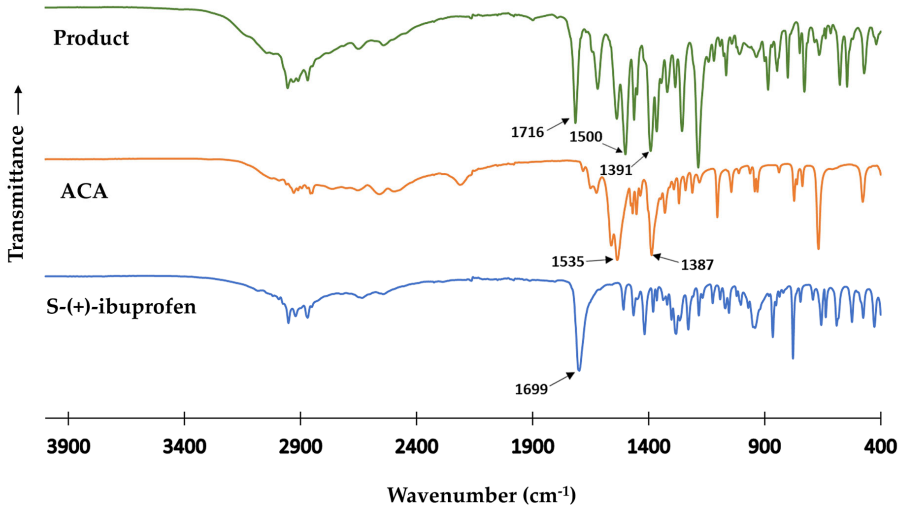

Figure 7. FTIR spectra of S-(+)-ibuprofen, ACA, and the product of their reaction.

While the carbonyl bond in pure S-(+)-ibuprofen was evident from the strong absorption at 1699 cm^{-1}, there was no carbonyl absorption band in the spectrum of pure ACA, since it is zwitterionic. Instead, this coformer displayed the expected strong asymmetric and symmetric carboxylate stretching bands at ν_{as} = 1535 cm^{-1} and ν_{s} = 1387 cm^{-1}, respectively. In the spectrum of the product, however, a carbonyl stretching band appeared at 1716 cm^{-1}, accompanied by strong carboxylate stretching bands with ν_{as} = 1500 cm^{-1} and

ν_s = 1391 cm^{-1}, respectively, which differed significantly from those displayed by pure ACA. These results indicated that the band with ν(C=O) = 1716 cm^{-1} in the spectrum of the product was due to the presence of a -COOH group in the coformer ACA, resulting from proton transfer from S-(+)-ibuprofen, which instead occurred in the product as the deprotonated S-(+)-ibuprofenate anion. Similar FTIR results from the analysis of the spectra of S-(+)-ibuprofen, TXA, and their corresponding product led to an analogous interpretation, indicating that this product is also a salt (Figure S5, Supplementary Materials).

3.3. Thermal Analysis

Figures S6 and S7 (Supplementary Materials) show the DSC and TGA curves for the two new salts, $(S\text{-}IBU)^-(ACA)^+$ and $(S\text{-}IBU)^-(TXA)^+$, which displayed relatively uncomplicated behaviors on heating, namely melting and subsequent decomposition. Sharp fusion endotherms in the DSC curves occurred at T_{peak} = 134 °C (melting range 128–138 °C) for $(S\text{-}IBU)^-(ACA)^+$ and T_{peak} = 181 °C (melting range 174–183 °C, with decomposition) for $(S\text{-}IBU)^-(TXA)^+$. It was noted, however, that for the latter salt, a mass loss of ~54% occurred between 135 and ~210 °C, corresponding to the calculated mass percentage (theoretical value: 56%) for $(S\text{-}IBU)^-(TXA)^+$ with 1:1 stoichiometry. The remaining TXA was a high-melting-point solid with an m.p. of ~300 °C [21]. The crystal structure of pure S-(+)-ibuprofen (CSD refcode JEKNOC12) is composed of hydrogen-bonded carboxylic acid dimers with no H-bonds between them, and consequently this API has a relatively low melting point, namely 49–53 °C [22]. The increased thermal stability associated with the salts of S-(+)-ibuprofen reported here could therefore be attributed to the extensive networks of charge-assisted hydrogen bonds that featured in their crystal structures described above.

3.4. Solubility Measurements in FaSSIF

To establish whether the alternative solid forms of S-IBU prepared in this study displayed any solubility advantages, the equilibrium solubilities of pure S-IBU; the two new salts $(S\text{-}IBU)^-(ACA)^+$ and $(S\text{-}IBU)^-(TXA)^+$; and that of a known cocrystal, S-IBU·benzamide [9] (re-synthesised and characterized in our laboratory for comparative purposes), were measured in FaSSIF (fasted-state simulated intestinal fluid) according to the procedure described in Section 2.8. A table listing the equilibrium concentrations of these four species at two pH values (2.0 and 6.5), as well as their solubility values in mg/mL, is presented in the Supplementary Material (Table S3). From this table, we noted that the relative solubilities of the four species did not differ significantly at a given pH.

4. Conclusions

As described in the Introduction, the literature on the solid state of the API S-(+)-ibuprofen (S-IBU) features a range of multi-component systems that contain this drug. However, given that S-IBU is a very effective non-steroidal anti-inflammatory drug, superior in many respects to the racemic form of ibuprofen, 'drug–drug' salts or cocrystals containing S-IBU are nevertheless rare. The salts described in the present study therefore represent new crystalline 'drug–drug' products that were based on exploiting the pharmacological properties of both S-IBU (for the relief of inflammation, pain, and fever) and the antifibrinolytics ACA and TXA (namely, arresting blood flow, which might result from the adverse ulcerative effects of S-IBU). Another novel feature of this study is the fact that the 'coformers' ACA and TXA selected for the 'drug–drug' synthesis study with S-IBU are zwitterions, ionic species that are seldom employed in this capacity. Accurate X-ray structures of the salts $(S\text{-}IBU)^-(ACA)^+$ and $(S\text{-}IBU)^-(TXA)^+$ were determined, and the strong hydrogen bonding interactions that stabilize them contribute to their superior thermal stability relative to untreated S-IBU. However, the assessment of the pharmacological effects of these salts has yet to be conducted in order to determine whether the notion of their potential pharmaceutical advantages expressed in this report may be verified.

Supplementary Materials: The following supporting information can be downloaded at: https://www.mdpi.com/article/10.3390/cryst13081222/s1, Figure S1: HPLC calibration curve, Figure S2: PXRD patterns of the starting components S-IBU and TXA, and those of the products obtained by liquid-assisted grinding, Figure S3: ^{1}H-NMR spectrum of $(S\text{-}IBU)^{-}(ACA)^{+}$, Figure S4: Experimental and calculated PXRD patterns for $(S\text{-}IBU)^{-}(TXA)^{+}$ and for $(S\text{-}IBU)^{-}(ACA)^{+}$, Figure S5: FTIR spectra of S-(+)-ibuprofen, TXA, and their product, Figure S6: DSC and TGA curves for $(S\text{-}IBU)^{-}(ACA)^{+}$, Figure S7: DSC and TGA curves for $S\text{-}IBU)^{-}(TXA)^{+}$, Table S1: HPLC gradient elution program, Table S2: Analysis of the ^{1}H-NMR spectrum of $(S\text{-}IBU)^{-}(ACA)^{+}$, Table S3: Solubility data for four solid forms of S-(+)-ibuprofen.

Author Contributions: Conceptualization, H.S.R., H.M.F. and M.R.C.; methodology, H.S.R., H.M.F. and C.E.-S.; validation, H.M.F., H.S.R. and C.E.-S.; formal analysis, H.S.R., H.M.F., C.E.-S. and M.R.C.; investigation, H.S.R., H.M.F. and C.E.-S.; resources, M.R.C.; data curation, H.S.R., H.M.F., C.E.-S. and M.R.C.; writing—original draft preparation, M.R.C. and H.M.F.; writing—review and editing, H.S.R., H.M.F., C.E.-S. and M.R.C.; visualization, H.M.F. and M.R.C.; supervision, M.R.C.; project administration, M.R.C.; funding acquisition, M.R.C. All authors have read and agreed to the published version of the manuscript.

Funding: This research received no external funding.

Data Availability Statement: The data presented in this study are available in the Supplementary Materials. In addition, the CSD deposition numbers for $(S\text{-}IBU)^{-}(ACA)^{+}$ and $(S\text{-}IBU)^{-}(TXA)^{+}$ are CCDC 2259078 and 2259079, respectively. The CIF files for these X-ray structures can be obtained free of charge via http://www.ccdc.cam.ac.uk/conts/retrieving.html, accessed on 4 July 2023 (or from the CCDC, 12 Union Road, Cambridge, CB2 1EZ, UK; fax: +44-1223-336-033; email: deposit@ccdc.cam.ac.uk).

Acknowledgments: M.R.C. thanks the University of Cape Town for access to research facilities.

Conflicts of Interest: The authors declare no conflict of interest.

References

1. Choquesillo-Lazarte, D.; Domínguez-Martín, A. Editorial: Multicomponent Pharmaceutical Solids. *Crystals* **2023**, *13*, 570. [CrossRef]
2. Gliszczyńska, A.; Sánchez-López, E. Dexibuprofen Therapeutic Advances: Prodrugs and Nanotechnological Formulations. *Pharmaceutics* **2021**, *13*, 414. [CrossRef] [PubMed]
3. Evans, A.M. Comparative Pharmacology of S(+)-Ibuprofen and (RS)-Ibuprofen. *Clin. Rheumatol.* **2001**, *20*, 9–14. [CrossRef] [PubMed]
4. Bonabello, A.; Galmozzi, M.R.; Canaparo, R.; Isaia, G.C.; Serpe, L.; Muntoni, E.; Zara, G.P. Dexibuprofen (S+-isomer ibuprofen) reduces gastric damage and improves analgesic and antiinflammatory effects in rodents. *Anesth. Anal.* **2003**, *97*, 402–408. [CrossRef] [PubMed]
5. Bolla, G.; Sarma, B.; Nangia, A.K. Crystal Engineering of Pharmaceutical Cocrystals in the Discovery and Development of Improved Drugs. *Chem. Rev.* **2022**, *122*, 11514–11603. [CrossRef] [PubMed]
6. Dexibuprofen: Uses, Interactions, Mechanism of Action | DrugBank Online. Available online: https://go.drugbank.com/drugs/DB09213 (accessed on 29 June 2023).
7. Friščić, T.; Jones, W. Cocrystal architecture and properties: Design and building of chiral and racemic structures by solid–solid reactions. *Faraday Discuss.* **2007**, *136*, 167–178. [CrossRef] [PubMed]
8. Berry, D.J.; Seaton, C.C.; Clegg, W.; Harrington, R.W.; Coles, S.J.; Horton, P.N.; Hursthouse, M.B.; Storey, R.; Jones, W.; Friščić, T.; et al. Applying Hot-Stage Microscopy to Co-Crystal Screening: A Study of Nicotinamide with Seven Active Pharmaceutical Ingredients. *Cryst. Growth Des.* **2008**, *8*, 1697–1712. [CrossRef]
9. Dash, S.G.; Thakur, T.S. Computational Screening of Multicomponent Solid Forms of 2-Aryl Propionate Class of NSAID, Zaltoprofen, and Their Experimental Variation. *Cryst. Growth Des.* **2021**, *21*, 449–461. [CrossRef]
10. Springuel, G.; Robeyns, K.; Norberg, B.; Wouters, J.; Leyssens, T. Cocrystal Formation between Chiral Compounds: How Cocrystals Differ from Salts. *Cryst. Growth Des.* **2014**, *14*, 3996–4004. [CrossRef]
11. Groom, C.R.; Bruno, I.J.; Lightfoot, M.P.; Ward, S.C. The Cambridge Structural Database. *Acta Cryst.* **2016**, *B72*, 171–179. [CrossRef] [PubMed]
12. Kleemiss, F.; Puylaert, P.; Duvinage, D.; Fugel, M.; Sugimoto, K.; Beckmann, J.; Grabowskya, S. Ibuprofen and sil-ibuprofen: Polarization effects in the crystal and enzyme environments. *Acta Cryst.* **2021**, *B77*, 892–905. [CrossRef]
13. Tilborg, A.; Springuel, F.; Norberg, B.; Wouters, B.; Leyssens, T. On the influence of using a zwitterionic coformer for co-crystallization: Structural focus on naproxen-proline cocrystals. *CrystEngComm* **2013**, *15*, 3341–3350. [CrossRef]

14. Al Rahal, O.; Williams, P.; Hughes, C.; Kariuki, B.; Harris, K. Structure Determination of Multicomponent Crystalline Phases of (S)-Ibuprofen and L-Proline from Powder X-ray Diffraction Data, Augmented by Complementary Experimental and Computational Techniques. *Cryst. Growth Des.* **2021**, *21*, 2498–2507. [CrossRef]
15. Cajaraville, J.P. Ibuprofen Arginate for Rapid-Onset Pain Relief in Daily Practice: A Review of Its Use in Different Pain Conditions. *J. Pain Res.* **2021**, *14*, 117–126. [CrossRef] [PubMed]
16. Markowska, A.; Markowski, A.R.; Jarocka-Karpowicz, I. The Importance of 6-Aminohexanoic Acid as a Hydrophobic, Flexible Structural Element. *Int. J. Mol. Sci.* **2021**, *22*, 12122. [CrossRef] [PubMed]
17. Liu, Q.; Geng, P.; Shi, L.; Wang, Q.; Wang, P. Tranexamic acid versus aminocaproic acid for blood management after total knee and total hip arthroplasty: A systematic review and meta-analysis. *Int. J. Surg.* **2018**, *54 Pt A*, 105–112. [CrossRef]
18. Prudovsky, I.; Kacer, D.; Zucco, V.V.; Palmeri, M.; Falank, C.; Kramer, R.; Carter, D.; Rappold, J. Tranexamic acid: Beyond antifibrinolysis. *Transfusion* **2022**, *62*, S301–S312. [CrossRef]
19. Nechipadappu, S.K.; Reddy, I.R.; Tarafder, K.; Trivedi, D.R. Salt/Cocrystal of Anti-Fibrinolytic Hemostatic Drug Tranexamic acid:Structural, DFT, and Stability Study of Salt/Cocrystal with GRAS Molecules. *Cryst. Growth Des.* **2019**, *19*, 347–361. [CrossRef]
20. Braga, D.; Maini, L.; Grepioni, F.; De Cian, A.; Félix, O.; Fischer, J.; Hosseini, M.W. Charge-assisted N-$H^{(+)}\cdots O^{(-)}$ and O-$H^{(+)}\cdots O^{(-)}$ hydrogen bonds control the supramolecular aggregation of ferrocenedicarboxylic acid and bis-amidines. *New J. Chem.* **2000**, *24*, 547–553. [CrossRef]
21. Gomes dos Reis, L.; Ghadiri, M.; Young, P.; Traini, D. Nasal Powder Formulation of Tranexamic Acid and Hyaluronic Acid for the Treatment of Epistaxis. *Pharm. Res.* **2020**, *37*, 186. [CrossRef] [PubMed]
22. Dexibuprofen | C13H18O2 | CID 39912—PubChem. Available online: https://pubchem.ncbi.nlm.nih.gov/compound/Dexibuprofen#section=Experimental-Properties (accessed on 29 June 2023).